Towards a discrete electronic transmission line as a musical harmonic oscillator

Kurijn Buys
Strange New Instruments
kurijn@gmail.com

Roman Auvray
LAM - D'Alembert
UPMC Univ Paris 06, UMR CNRS 7190,
Paris, France
auvray@lam.jussieu.fr

ABSTRACT

In analogy with strings and acoustic pipes as musical harmonic oscillators, a novice electronic oscillator is considered. The equivalent circuit of a discrete representation of strings and pipes, which takes the form of a discrete transmission line, is constructed with real electronic components. The proposed model includes the "equivalent series resistances", which seems to be the only relevant default for both capacitors and inductors for this application. In an analytical approach, the complex wave number is derived, allowing the study of both the wave's dispersion and attenuation in function of frequency and resulting in recommended and critical component values. Next, components are selected for a first eight-node prototype, which is numerically evaluated and then practically constructed and measured. The results prove a good match between theory and practice, with five distinguishable modes in the entrance impedance. A new prototype design is planned, which is expected to have much improved quality factors.

1. INTRODUCTION

The analogue dynamic theories between acoustics and electronics, allow an "equivalent electronic circuit" representation of linear oscillating mechanisms. A well-known example is the simple spring-mass system that can be represented by an equivalent capacitor-inductor or "LC" oscillator. While this concept is usually applied to facilitate calculations it also can serve as a source of inspiration to design new musical electronic circuits. The discrete ideal string or acoustic pipe representation consists of concatenated spring-mass systems. This leads to the idea to construct an equivalent circuit of this so called "discrete transmission line" model, with real components that could operate as a string or pipe. Such a circuit allows electronic charges to propagate and reflect at open or shorted endings as boundary conditions, which results in an electronic harmonic oscillator.

While the proposed electronic resonator is a first order approach of both a string and pipe, it is just the difference between these acoustic examples that illustrates the great variety in timbre and musical expression. Therefore, the proposed electronic sound propagative medium is expected to offer new potentials in this regard. The more detailed model of the electronic resonator such as electric losses and nonlinearities and the musician's access to control the instrument, will bring along its proper (unheard) character. Also, the electric medium allows its own transform possibilities (we can think of interaction with magnets, adding external circuits, easily switching between boundary conditions, designing a broad variety of mouthpiece models,...).

Historically, it is custom to use equivalent electrical circuits to study sound transmission through ducts under low frequency assumptions. For instance, every acoustic publication usually presents the Helmholtz resonator along with its equivalent electrical circuit [1]. A panel of "duct accidents", such as constrictions or tone holes, can also be described using equivalent electrical circuits if the different elements are assumed to interact by simple in- and outputs only. This is the lumped description that is opposed to an integral approach.

Passive [2, 3], as well as active [4], studies of musical instruments also benefited from their equivalent electrical description. Following the classical description of sound production as a coupling between an exciter, eventually non-linear, and a resonator [5, 6], attempts have been made to model sound production with electrical circuits only [7]. Despite the theoretical studies that have been performed, no experimental, and academical, work seems, to the authors' knowledge, to be done on this issue, which could be explained by the only recently available low resistive capacitors.

As for the design objectives, as usual for musical instruments, a very resonant and harmonic system is desired. This allows for large dynamics and a long sustained sound with a wide timber variety. The low inharmonicity objective is also motivated by the fact that for self-sustained operation (like winds), the pitch of second register notes, mainly determined by the second harmonic, will be in better accordance with the first register note.

While several plucked and self-sustained excitation mechanisms can be imagined, this part of the complete electronic instrument is not treated in this article.

2. THEORETICAL STUDY

2.1 Deducing an appropriate model

Considering existing harmonic resonators such as strings and pipes, we can apply a discretization on a ideal model to become a finite element approximated representation consisting of N concatenated equal valued springs and masses leading to N normal modes. This can be interpreted as a two-terminal circuit which has both a Thévenin and Norton equivalent circuit form [8]. In the case of a string, the former translates force and velocity respectively as the voltage and current, while the springs and masses respectively relate to capacitors and inductors. The Norton equivalent has opposite relations but is further not concerned in our study. Using real components for this discrete transmission line, their own non-ideal characteristics will come into play, so that an adapted model is needed that takes in these relevant artefacts.

A first thing to note is that the discretization at the boundaries, using a first order approach, causes the inductor at a shorted boundary to be of half the inductance of the "in-line" inductors, and similarly, a half-valued capacitor is used at an open boundary. We will concentrate the study on a situation with an open entrance and shorted end boundary conditions, but similar results apply for all other situations as the electrical open and shorted conditions preserve the electrical charge and thus are acceptable approximations of the Dirichlet and Neumann conditions, respectively. While in mechanics and acoustics a considerable energy loss is typical at the boundaries, partly to make the instrument audible, in this electrical case, a high impedance connection can be used to pick up the signal and amplify the sound.

In order to analytically and numerically study the model, we look for an equivalent circuit that includes relevant component artefacts.

Most of the real capacitor defaults are not of importance for our application. The systems linearity allows a study and use at low voltages, under the maximum operation or "breakdown" voltage, and avoiding ripple currents. The inherent inductance and parallel conductance are negligible at audio frequencies [9]. It is only the "Equivalent Series Resistance" (ESR) that is of relevance. This factor is usually specified at $100\ kHz$ and, according to datasheet observations, increases about 5 to 100 times at $100\ Hz$, which depends on the capacitor type.

The real inductor's magnetic saturation, parasitic capacitance and core hysteresis can be neglected for the same reasons. Besides inductance, it is also only the ESR (or "DCR" in datasheets), that plays a role in our application [10].

For the same type of capacitor (materials, voltage rating,...) and inductor (wire type, core material and dimension,...), the ESR, R_C and R_L, are related to their capacitance and inductance [9, 10], respectively, by:

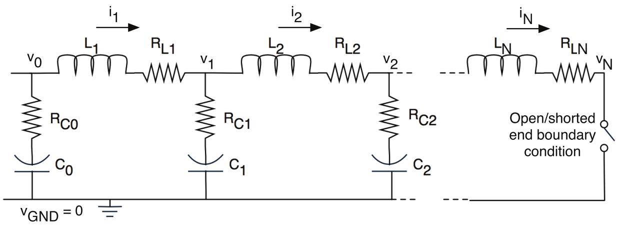

Figure 1. Outline of the discrete transmission line with the appropriate component models

$$\begin{cases} R_C = ESR = \gamma_C / C \\ R_L = DCR = \gamma_L \sqrt{L} \end{cases} . \tag{1}$$

For different inductors, the remaining resistive factor γ_L stays around the order of $1\ \Omega/\sqrt{H}$, while the resistive capacitor factor γ_C takes the unit of seconds and varies in the orders of $[10^{-7} - 10^{-3}]\ s$ depending on the capacitor type and design.

Everything together, the appropriate model is presented in figure 1. It should be noted that all inductances L_i are equal except for $L_N = L_{i \neq N}/2$. The same applies for resistor R_{Li}, capacitor C_i and resistor R_{Ci} while $R_{LN} = R_{i \neq N}/\sqrt{2}$, $C_1 = C_{i \neq N}/2$, and $R_N = 2R_{i \neq N}$. This model is close to the classical electrical transmission line model based on the Telegrapher's equations [11]. However, here the capacitor's ESR is of importance, rather than its parallel conductance G.

2.2 Analytical approach

We develop a mathematical approach to study the proposed transmission line that partly corresponds to the typical transmission line derivation [11, 12].
First we describe the wave propagation in an infinite "discrete" transmission line. Referring to figure 1 and applying elementary circuit analysis to each node we obtain a set of basic circuit equations that after a Fourier transform directly are expressed in the frequency domain as follows

$$\begin{cases} V_{n+1}(\omega) = V_n(\omega) - Z_s(\omega)\ I_{n+1}(\omega) \\ I_{n+1}(\omega) = I_n(\omega) - Y_p(\omega)\ V_n(\omega) \end{cases} , \tag{2}$$

with V_i and I_i the voltage and current in the corresponding nodes, and

$$\begin{cases} Z_s(\omega) = R_L + j\omega L & \text{series impedance} \\ Y_p(\omega) = \frac{1(\omega)}{R_C + \frac{1}{j\omega C}} & \text{shunt (parallel) admittance} \end{cases} . \tag{3}$$

To solve equations (2), we first can cast this array of coupled inhomogeneous equations in the form of a set of coupled, homogeneous algebraic equations that evidence a simple set of solutions, which may be written in the form:

$$\begin{cases} V_{n+1}(\omega) = V_n e^{-\Gamma(\omega)} \\ I_{n+1}(\omega) = I_n e^{-\Gamma(\omega)} \end{cases} , \tag{4}$$

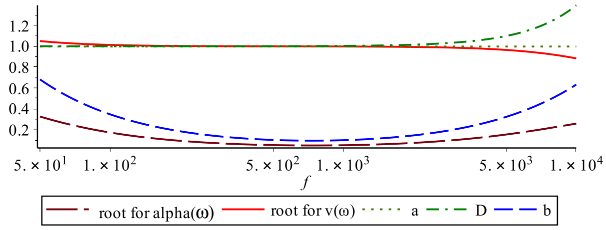

Figure 2. Frequency evolution of the losses contribution roots and its coefficients, for the typical component values: $\frac{\gamma_L}{\sqrt{L}} = 213\ s^{-1}$, $\frac{1}{\gamma_C} = 10^5\ s^{-1}$.

where Γ is the complex wave number. If these "constant phase solutions" are to be valid solutions, the nodal phase constant $\Gamma(\omega)$ must satisfy the equation:

$$Z_s(\omega)Y_p(\omega) = e^{-\Gamma(\omega)} + e^{\Gamma(\omega)} - 2. \quad (5)$$

This results in the dispersion relationship for a discrete, uniform transmission line:

$$\Gamma(\omega) = 2\ \text{arcsinh}\left(\frac{\sqrt{Z_s(\omega)\,Y_p(\omega)}}{2}\right). \quad (6)$$

For a lossless case, we can write $Z_s(\omega)\,Y_p(\omega) = -\omega^2 LC$. $\Gamma(\omega)$ is purely imaginary so that no evanescent waves appear and the nodal phase velocity $v_\varphi(\omega) = \frac{\omega}{Im(\Gamma(\omega))}$ remains constant at low frequencies. v_φ only decreases by 5% at $\omega = \omega_{0ll} = \frac{1}{\sqrt{LC}}$, the resonant frequency of a single lossless LC oscillator, which explains that a finer discretization reduces this "numerical dispersion".

Considering the losses, the wave number is complex and also comprises evanescent waves, described by a nodal attenuation coefficient $\alpha(\omega) = Re(\Gamma(\omega))$. Using eqs. (6) and (3), we obtain:

$$\begin{cases} v_\varphi(\omega) = \dfrac{\omega}{\text{arcsinh}\left(\omega\sqrt{LC}\sqrt{\frac{a+\sqrt{a^2+b^2}}{2D}}\right)} \\ \alpha(\omega) = \text{arcsinh}\left(\omega\sqrt{LC}\sqrt{\frac{-a+\sqrt{a^2+b^2}}{2D}}\right) \end{cases}, \quad (7)$$

where (using the "equal type" formulations (1))

$$\begin{cases} a = 1 - R_L R_C \frac{C}{L} = 1 - \frac{\gamma_L \gamma_C}{\sqrt{L}} \\ b = \frac{R_L}{\omega L} + \omega R_C C = \frac{\gamma_L}{\omega\sqrt{L}} + \omega\gamma_C \\ D = (\omega R_C C)^2 + 1 = (\omega\gamma_C)^2 + 1 \end{cases}. \quad (8)$$

Considering a constant nodal velocity and maintaining the same type of components, it is clear that L/C should be chosen as high as possible to reduce the influence of losses. The order of γ_L is about $1\ \sqrt{\Omega/s}$, γ_C lies between $[10^{-7} - 10^{-3}]\ s$ and L will have an order of $[10^{-6} - 10^{-2}]\ H$, so that a number of frequency values can be derived that will indicate critical lossy zones.
The frequency evolution of the roots and their coefficients is presented in figure 2. While a remains constant over frequency and near to 1, the coefficients b and D vary over frequency.

For $\omega < \frac{\gamma_L}{\sqrt{L}} = [3 - 300]\ s^{-1}$, b increases rapidly so that both the roots for v_φ and α increase.

When ω approaches $\frac{1}{\gamma_C} = [10^3 - 10^7]\ s^{-1}$, b also increases , but D raises by ω^2.
In the case of v_φ, the nominator increment is slower than D, so that the root reduces, and thus the phase velocity increases (counteracting on the numerical dispersion).
For $\alpha(\omega)$, the nominator first increases faster than D, increasing the root to a maximum close to $\omega = 1/\gamma_C$, where D will prevail and decrease the root again. However, the ω factor in the expression of α increases the attenuation factor with frequency.

When we now consider a finite number of N nodes with an open entrance and a shorted end condition, standing waves will appear. The near to ideal boundary conditions guarantee a simple reflection coefficient that only holds the medium losses, contained in the complex wave number: $R(\omega) = -e^{-2\Gamma N}$. Also in analogy with an acoustic cylinder (neglecting radiation) [13], the nondimensional entrance impedance can be derived as follows:

$$Z_e/Z_c = \frac{1 + R(\omega)}{1 - R(\omega)} = \tanh\left(\Gamma N\right), \quad (9)$$

with $Z_c = \sqrt{Z_s/Y_p}$, the characteristic impedance for a transmission line, which is close to the real constant $\sqrt{L/C}$ for $\frac{R_L}{L} \ll \omega \ll \frac{1}{R_C C}$, where losses are small [14].

The entrance impedance Z_e is characterized by a number of modes who's coefficients can be related to the wave number components (see Eq. (7)). The (anti-)resonant frequencies $\omega_n = 2\pi n v_\varphi/2N$ and $\omega_n = 2\pi(2n-1)v_\varphi/4N$ illustrate the direct relation of the inharmonicity to the change in phase velocity $v_\varphi\omega_{0ll}$ (which is constant when perfectly harmonic). These frequencies indicate the extrema of the impedance modulus, that depend on the attenuation coefficient α:

$$a_{(M,m)n} \approx \tanh\left(\alpha(\omega_n)N\right)^{\mp 1} \approx \left(\alpha(\omega_n)N\right)^{\mp 1}, \quad (10)$$

where the negative exponent applies to the maxima M and the positive one to the minima m.
The modal quality factor is proportional to the maxima but increases with the frequency, and is independent of N for low frequencies:

$$Q_n \approx a_{(M)n}\omega_n \frac{N}{2v_\varphi(\omega)}, \quad (11)$$

For equal components, apart from the $\alpha(\omega)$'s root deviation, the number of nodes does not affect both amplitude and quality factors of the harmonic series.

It is interesting to study the case where a fundamental frequency is maintained while increasing the number of nodes by choosing the same inductors and smaller capacitors of the same type. When doubling the number of nodes for example, we choose $C/4$ for the new capacitors, the coefficients in Eq. (8) remain equal so that the only change in numerical dispersion decreases the inharmonicity. As the attenuation coefficient is halved, both the a_n and Q_n remain equal. This means that a fine discretization can be applied with only the advantage of enhanced harmonicity.

To resume, apart from a preferable high L/C factor; concerning the inductor, $\frac{\gamma_L}{\sqrt{L}}$ should be chosen low enough under the fundamental frequency of the resonator, especially for (first register) self-sustained oscillation where the first resonant peak should be relatively high. As for the capacitor, $\frac{1}{\gamma_C}$ should be chosen as high as possible to promote a soft spectral decay of the impedance peaks.

To obtain sounds, an exciter will be needed. A simple initial voltage condition is sufficient to model a simple pluck-type excitation. However, for self-sustained control (which would be preferable if the resonator is very lossy), a convenient exciter model would need components that supply a voltage to current ratio in the same order as the characteristic impedance, just as for acoustic self-sustained mechanisms [5]. For now, we disregard the exciter part and concentrate on the independent validation of the electronic resonator.

3. STUDY OF A FIRST PROTOTYPE

In this section we will discuss the conception and measurement of a concrete transmission line. The aim is to compare the theory to a first practical prototype to allow more specific designs later on. We arbitrary choose an eight node line with ω_{0ll} around $2\pi 1200$ to become a fundamental frequency of about 230 Hz.

3.1 Selecting appropriate components

3.1.1 Inductors

The ESR of inductors depends on to the wire length and thickness [14]. Therefore, the variation on γ_L for a same cable thickness depends on the core design and permeability to the extent of space for windings. A classical inductor may have γ_L as low as 1.5. Special core materials, such as those used in "common mode chokes", can lower this value down to 0.5, but the core becomes easily magnetically saturated so that a linear use allows a very limited coil current. We could neglect this amplitude related aspect, which even might evoke a desirable saturation effect on the sound when experimenting with higher amplitudes later on. However, These coils have close windings so that the increased inherent capacitance can slightly decrease the coil reactance at high frequencies. For these reasons we opt for a standard coil type for our first prototype.
We choose a 22 μH Bourns $2305 - RC$ inductor with $R_L = 7\ m\Omega$ and $\gamma_L = 1.5$.

3.1.2 Capacitors

Many industrial applications have promoted the design of low ESR capacitors, but none of them are specifically designed for the audio domain, which explains the poor concerning information in datasheets. We consider three suitable types [15]:

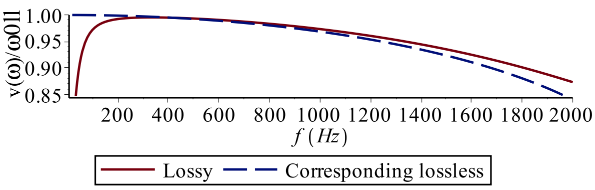

Figure 3. Evolution of the phase velocity relative to ω_{0ll} for the lossy and the corresponding lossless case.

- Polymers (dry electrolyte), with typical capacities of $[10{-}3000]\mu F$ and $\gamma_C = [10^{-6}{-}10^{-4}]\ s$ at 100 Hz.
- Ceramics, where the "MLCC" ceramic chips have the lowest ESR, about 1/3 of Polymers. However, it seems that ESR rapidly increases towards the audio domain and little information is available. Their capacities range between $[1\ pF - 100\ \mu F]$ but for the very low ESR $NP0$ type C is maximum 0.1 μF. It should be noted that these components are susceptible to contact noises due to their piezo-electric side-effect.
- Film capacitors, especially the Polypropylene type have very low ESR. But as the ceramics, no audio frequency information is provided. The capacity ranges between $[10\ pF - 1\ mF]$.

To obtain meaningful conclusions between theory and practice, we prefer a fully quantified Polymer capacitor. We choose a Nichicon $E5$ series 820 μF, 6.3 V capacitor with $R_C = 18\ m\Omega$ at 100 Hz (descending to 5 $m\Omega$ at 100 kHz) and $\gamma_C = 1.5 \times 10^{-5}$.

3.1.3 Conclusion

The resulting lossless single LC frequency is $\omega_{0ll} = 2\pi\ 1185$. While these components are far from the most optimal choice, the results will allow a clear comparison to the theory. The characteristic impedance is relatively low: $\sqrt{L/C} = 0.16\ \Omega$. $\frac{\gamma_L}{\sqrt{L}} = 2\pi\ 51$ is below the fundamental frequency of about 230 Hz and $\frac{1}{\gamma_C} = 2\pi\ 10^4$ lies far above ω_{0ll}.
Using equations (7), the frequency evolution of the phase velocity and attenuation coefficient is calculated for this case.
Figure 3 represents the evolution of the phase velocity relative to the constant lossless velocity, so that a constant value of 1 would indicate an absence of inharmonicity. A corresponding lossless case is added to illustrate the effect of the numerical dispersion. As predicted, below $\omega = \frac{\gamma_L}{\sqrt{L}}$ the velocity drops and at high frequencies, the dispersion due to losses counteracts on the numerical dispersion.
Figure 4 shows $\alpha(\omega)$ represented by the real part of Γ. The globally increasing progression is explained by the ω factor in its expression.

The resulting entrance impedance, as calculated by equation (11) is shown in figure 8, together with the numerical and measured curves.

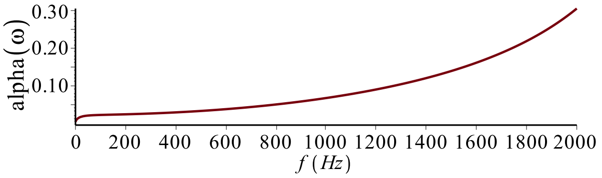

Figure 4. Evolution of the attenuation coefficient $\alpha(\omega)$ over frequency.

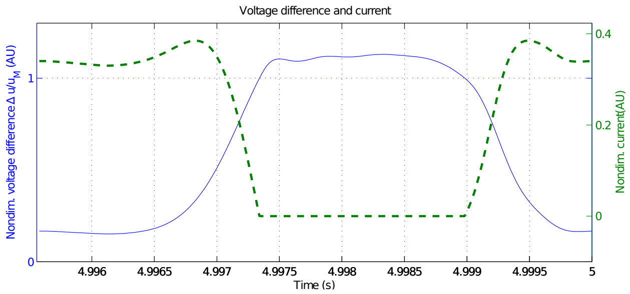

Figure 5. Temporal input voltage and current signals during a self-sustained operation with a nondimensional input voltage or “mouthpiece pressure” of 0.65.

3.2 Numerical simulation

Before the final construction, we used Matlab and Simulink to perform a numerical simulation on the proposed model with the chosen components. This allows to observe the eventual influence of aspects neglected in the analytical study, such as the approximated discretization at the borders, the inductor’s inherent capacitance C_L and the capacitor’s parallel conductance G. The entrance impedance curves are presented in figure 8.

We also added a single reed exciter model [16–18] and we empirically confirmed a self-sustained operation. The resulting input current and voltage signals are shown in figure 5 and the spectrum of the latter is represented in figure 6.

The nondimensional oscillation threshold is found to be minimum 0.6, which is above the usual clarinet thresholds [13], what can be explained by the relatively low modal amplitudes and quality factors and the prominent inharmonicity of our resonator. However, the spectrum, waveform and sound are similar to a simulated clarinet in the “beating reed” regime [16]. The fundamental frequency is found at $f_0 = 225.2\,Hz$, which is slightly below $230.7\,Hz$, the frequency of the first resonant peak. This may be clarified by the numerical dispersion that turns down the frequency of the higher resonant peaks.

3.3 Concrete realization and measurement

An actual realization of the proposed transmission line is constructed and is depicted in figure 7. Two equally valued capacitors are put in series to obtain the needed half-valued capacitance at the open entrance boundary. By measuring the voltages surrounding an additional appropriate resistance put in series with the transmission line entrance and

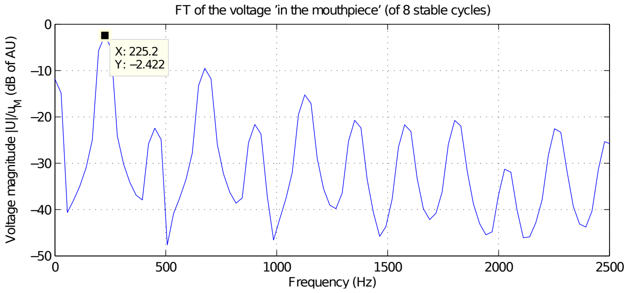

Figure 6. Spectrum of the input voltage signal with a nondimensional input voltage of 0.65.

Figure 7. First prototype of the discrete harmonic transmission line.

applying a voltage sweep, both the input voltage and current can be measured, so that the entrance impedance can be derived. The result is added to figure 8 and discussed in the next paragraph.

3.4 Theoretical and measured Z_e comparison

Figure 8 shows the spectral modulus and argument of the analytical, numerical and measured entrance impedances of the first discrete transmission line prototype with a shorted end condition. An open end condition is also verified and results in similar characteristics, but for even harmonics.

The analytical approach results in an entrance impedance with four clearly visible modes. The fundamental frequency is found at $f_0 = 230.7\,Hz$. The plotted lossless harmonics confirms the earlier shown inharmonicity curve: the second impedance peak is still very close to $3 \times f_0$, and later peaks diverge more and more downwards.

The first four nondimensional amplitude peaks are foud at $a_0 = 5.3$, $a_1 = 3.1$, $a_2 = 1.8$, $a_3 = 1.3$. And the corresponding modal quality factors are $Q_0 = 5$, $Q_1 = 7.2$, $Q_2 = 7.0$, $Q_3 = 6.6$. The quality factor is inversely related to the damping ratio $\zeta = \frac{1}{2Q}$, which should be smaller than 1 to obtain an underdamped system. While that condition is satisfied, this order of damping ratios only allows very short free oscillations, so that a self-sustained use is advised to obtain sounds. To compare with musical acoustic examples, the quality factor of clarinets lies between $10 - 50$ and wooden soundboards have their Q between $10 - 150$, while those of strings vary between $100 - 10^4$ [19].

Comparing the numerical with the analytic curves, we see that a very good match is obtained. This is found to be independent of the additional properties, C_L and G, of the concerned components.

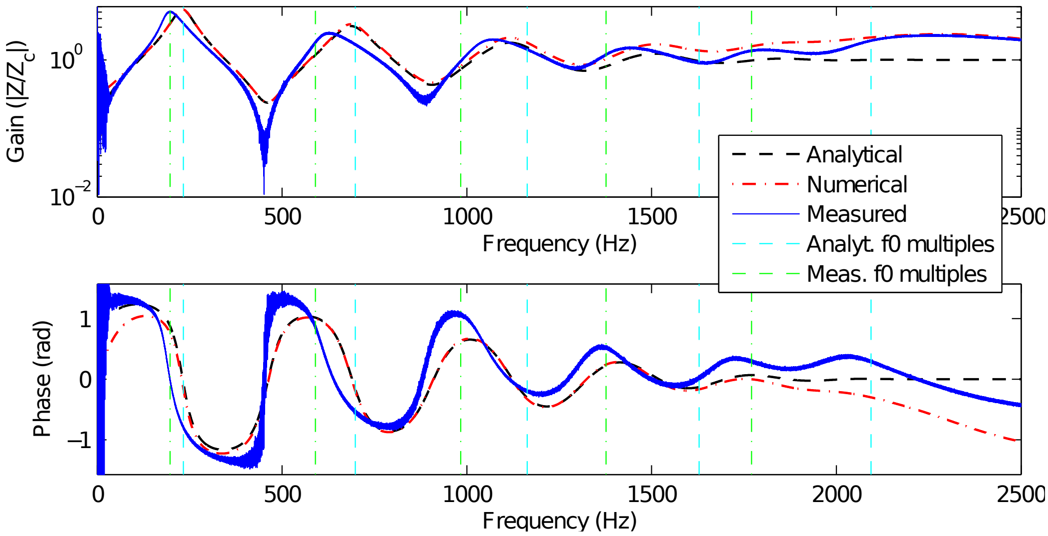

Figure 8. Input impedances of analytical, simulated and measured transmission lines.

Also the measured impedance is close to both predictions. At first sight, we observe an upwards inharmonicity. However, it is likely an actual higher R_L value that brings down the f_0 to 196.7 Hz. The amplitudes at the resonant frequencies and the quality factors closely correspond, while the anti-resonant peaks at low frequencies seem to descend more. Also, unlike the analytical and numerical approach a fifth harmonic is visible.

4. CONCLUSION AND PERSPECTIVES

The conception of a new electronic harmonic resonator with musical potentials is proved to be realizable. The measured entrance impedance of such a discrete transmission line with eight nodes is found to be very similar to the analytical and numerical approaches that use the corresponding datasheet values. This means that apart from capacitance and inductance, only the equivalent series resistance of both capacitors and inductors is to be considered for the design.

The lack of relevant ESR information in the audio frequency domain made us choose components with rather low characteristic impedance. However, more experimental models can be constructed that will likely feature much higher relative amplitudes and quality factors. Such an optimized model is already under construction, using eight 20 mH inductors and 1 μF film capacitors to obtain about the same fundamental frequency, a more convenient characteristic impedance of $Z_c = 140\,\Omega$ and roughly estimated quality factors of around 300! However, as it concerns "common mode" inductors, the current ratings are very low, especially for an additional direct current flux, so that a wind instrument design might be out of the question.

To cope with the numerical dispersion, we could add an adapted circuit at one of the boundaries that will introduce an opposite dispersion. However, as theoretically shown, increasing the node density, an equal relative losses and less dispersive model can be obtained by choosing the same inductors and smaller capacitors of the same type. This also is of interest when considering the perspective to play higher notes by moving the end boundary condition to a reduced number of nodes, just as releasing a key on a wind instrument...

Another perspective is the addition of electric circuits acting as convenient nonlinear exciters. These can be based on models of (single, double, free, lip or "flute") reeds, a bowing exciter [5, 19] or any other nonlinear relation that will result in a self-sustained oscillation. It would be desirable to use circuits with the same simplicity as the transmission line. However, equivalent circuits are not guaranteed for any nonlinear system. We think about FET's that might provide a single-reed mechanism equivalent, and also valves are considered, as they are reputed for their pleasing effect on sound.

5. REFERENCES

[1] A. D. Pierce, *Acoustics, an Introduction to its Physical Principles and Applications*. McGraw-Hill, 1981.

[2] J. W. Coltman, "Resonance and Sounding Frequencies of the Flute," *J. Acoust. Soc. Amer.*, vol. 40, pp. 99–107, 1966.

[3] D. H. Lyons, "Resonance frequencies of the recorder (English flute)," *J. Acoust. Soc. Amer.*, vol. 70, no. 5, pp. 1239–1247, 1981.

[4] A. W. Nolle, "Flue organ pipes: Adjustments affecting steady waveform," *J. Acoust. Soc. Amer.*, vol. 73, pp. 1821–1832, 1983.

[5] M. E. McIntyre, R. T. Schumacher, and J. Woodhouse, "On the oscillations of musical instruments," *J. Acoust. Soc. Amer.*, vol. 74, no. 5, pp. 1325–1345, 1983.

[6] B. Fabre and A. Hirschberg, "Physical Modeling of Flue Instruments: A Review of Lumped Models," *Acust. Acta Acust.*, vol. 86, pp. 599 – 610, 2000.

[7] J. W. Coltman, "Jet drive mechanisms in edge tones and organ pipes," *J. Acoust. Soc. Amer.*, vol. 60, pp. 725–733, 1976.

[8] D. Johnson, "Scanning Our Past - Origins of the Equivalent Circuit Concept: The Voltage-Source Equivalent," 2003.

[9] F. Mazda, *Discrete Electronics Components*. Cambridge University Press, 1981.

[10] A. Williams and F. Taylor, *Electronic filter design handbook*, ser. McGraw-Hill Handbooks. McGraw-Hill, 2006.

[11] R. V. Jones, "Transmission line theory," *Harvard University*, 2002.

[12] K. Nalty, "Transmission Lines, Stacked Insulated Washers Lines, Tesla Coils and the Telegrapher's Equation," 2008.

[13] J.-P. Dalmont, J. Gilbert, J. Kergomard, and S. Ollivier, "An analytical prediction of the oscillation and extinction thresholds of a clarinet," *Journal of the Acoustical Society of America*, vol. 118, no. 5, pp. 3294–3305, Nov. 2005.

[14] F. Ulaby, *Fundamentals of Applied Electromagnetics*. Pearson Educación, 2007.

[15] J. Wright, "Low ESR Capacitors," *Electro Sonic - E-Magazine*, 2004.

[16] K. Buys and C. Vergez, "A hybrid reed instrument: an acoustical resonator with a numerically simulated mouthpiece," *Acoustics 2012*, 2013.

[17] T. A. Wilson and G. S. Beavers, "Operating modes of the clarinet," *J. Acoust. Soc. Amer.*, vol. 56, pp. 653–658, 1974.

[18] A. Hirschberg, "Aero-acoustics of wind instruments," in *Mechanics of Musical Instruments*, J. K. A. Hirschberg and G. Weinreich, Eds. Wien: Springer, 1995.

[19] A. Chaigne and J. Kergomard, *Acoustique des instruments de musique*. Belin, 2008.